"Risk-based Probabilistic Small-disturbance Security Assessment of Power Systems"

R. Preece, J.V. Milanović

IEEE Transactions on Power Delivery, vol. 30, issue 2, pp. 590-598, 2014

Digital Object Identifier: 10.1109/TPWRD.2014.2301876

Risk-based Small-disturbance Security Assessment of Power Systems

R. Preece, *Member, IEEE*, and J. V. Milanović, *Fellow, IEEE*

***Abstract*—This paper presents a risk-based Probabilistic Small-disturbance Security Analysis (PSSA) methodology for use with power systems with uncertainties. This novel addition to existing Dynamic Security Assessment (DSA) techniques can be used to quantify the small-disturbance stability risks associated with forecasted operating conditions. This approach first establishes the probability density functions (*pdfs*) for the damping of the critical oscillatory electromechanical modes by modeling the stochastic variation of system uncertainties such as loading levels, intermittent generation sources, and power flows through Voltage Source Converter High Voltage Direct Current (VSC-HVDC) lines. The produced *pdfs* are then be combined with severity measures (either simple risk matrices or continuous functions) in order to quantify the risk of stability issues for the system associated with the forecasted operating scenario. Additionally, the PSSA is used to establish risk-based operational limits and the concept of a probabilistic security margin is introduced to more accurately represent the probabilistic operation of uncertain power systems. The proposed techniques are demonstrated using a multi-area meshed power system incorporating two VSC-HVDC systems, one of which is connected to a large wind farm.**

***Index Terms*—dynamic security assessment, electromechanical modes, security margin, small-disturbance stability, uncertainty, VSC-HVDC.**

I. Introduction

THE drive for greater efficiency, economics and energy security is resulting in the desire for greater utilization of current power system assets. The increase seen in the number of intermittent renewable energy sources and new types of system load is introducing more uncertain system parameters which subsequently lead to more variable operating conditions. The effects of these uncertainties must be thoroughly explored, and the risks introduced with respect to power system stability should be quantified.

Power system operators regularly perform security analysis to ensure that the network is not operated outside of tolerable limits. These limits can cover a wide variety of facets of power system operation, but typically focus on static phenomena such as line overloads, voltage limit excursions, and voltage stability margins [1]–[3]. In addition to these important factors, Dynamic Security Assessment (DSA) is required in order to identify and mitigate for possible dynamic system problems which may otherwise lead to wide-spread issues and potentially to system collapse.

Transient stability security assessment has typically been focused on the fast detection and calculation of suitable restorative control and protection schemes once the disturbance has occurred [4]–[6]. This is due to the fact that the consequences of large transient disturbances are extremely dependent on incident-specific uncertainties – such as fault location, fault type, fault clearing time, and the operating point at the time of the incident. In general, these transient stability predictors use classification techniques to identify whether evolving system conditions recorded online with Phasor Measurement Units (PMUs) will lead to instability based on large sets of training data simulated offline [5], [6]. Considering system variability, analytical linearized techniques have been used to accurately determine the probability distributions of power system critical clearing times based on loading uncertainties [7].

Small-disturbance stability relates to the ability of a power system to maintain stability following the small variations that naturally and continuously occur in practical power systems. As synchronous machines regain stability following disturbances, oscillations are seen in their rotor speeds, resulting in power oscillations throughout the system. Low frequency inter-area electromechanical oscillations are inherent in all large power systems [8], and in many cases the use of high generator exciter gains to improve the transient recovery of power systems has exacerbated small-disturbance stability concerns [9]. Unlike transient stability, small-disturbance stability is not dependent on the nature of the disturbance and can therefore be investigated using a probabilistic risk-based approach which accounts for system uncertainties. As complex conditions evolve within power systems, it is possible for underlying oscillations to become poorly damped or even unstable which can lead to equipment disconnection and eventual system collapse.

A Small-disturbance Security Assessment (SSA) tool has been presented in [10] where advanced computational algorithms are used to complete deterministic studies. It has been developed in order to determine operational guidelines which will alleviate power oscillation damping problems within power systems. However, the deterministic approach may fail to accurately represent the true system security levels as the increasing levels of uncertainty are not considered. The development of a Probabilistic SSA (or PSSA) will allow these variations to be incorporated into the assessment and therefore ensure that the system risks are correctly quantified.

This work was supported in part by the Research Councils UK, through the HubNet consortium (grant number: EP/I013636/1).

R. Preece and J.V. Milanović are with the School of Electrical and Electronic Engineering, The University of Manchester, PO Box 88, Manchester, M60 1QD, UK. (email: robin.preece@manchester.ac.uk, milanovic@manchester.ac.uk).

The area of risk-based small-disturbance stability analysis has received limited research effort with notable contributions towards probabilistic methods found [11]–[15]. In [11], the benefits of using a probabilistic approach to establish modal positions are outlined, however methods presented do not include further risk analysis. The work presented in [12] utilizes tetrachoric series in order to generate a probabilistic stability region for a power system. This work is limited in its assumption that all electromechanical modes can be described by a multivariate normal distribution which does not hold for non-linear power systems (as shown by the results presented in this paper). In [13]–[15], variations in the probability distributions of mode damping are investigated. However as with [11], the research does not evaluate *risk* in terms of both probability and severity, focusing purely on the probability of instability. The work within this field has focused upon the probabilistic techniques employed but has not completed risk analysis which considers *the severity* of the resultant conditions. Furthermore, measures of small-disturbance stability risk have not been used to establish meaningful operational limits which can guide system operation. Some initial work in this area has been published by the authors in [16] in which it was shown that risk measures can be formulated to assess small-disturbance stability issues.

This paper builds upon the previously discussed research to present a novel risk-based Probabilistic Small-disturbance Security Assessment methodology, demonstrated using a large mixed AC/DC power system. The PSSA is used to quantify the risk associated with forecasted loading scenarios by considering both the *stochastic uncertainty* in precise loading values, intermittent energy sources and power flows through Voltage Source Converter High Voltage Direct Current (VSC-HVDC) lines, and the *severity* of resultant power oscillations. Additionally, these proposed techniques are used for the first time to establish risk-based forecast power flow limits that will ensure that acceptable risk levels are not exceeded. The new concept of a Probabilistic Security Margin is introduced to represent the statistical nature of the standard security margin when accounting for system variability. Importantly, the methods and ideas presented within this work can be easily customized based upon the technical and regulatory framework under which any power system is operated.

II. Risk-based PSSA Methodology

The PSSA is completed by performing multiple linearisations of the power system whilst modeling the stochastic variation of the system uncertainties. These simulations are used to determine the probability density functions *(pdfs)* for the critical mode damping values on which the risk analysis is based. The proposed methodology can be summarized as follows:

(i) Establish mathematical descriptions of the system uncertainties (using historical or forecast data where available).

(ii) Simulate a large number of operating scenarios and perform deterministic studies on these samples to calculate details about critical system oscillations.

(iii) Determine the *pdf* for the critical mode damping from the collected data.

(iv) Select a *severity* measure and use this to quantify the system risk of small-disturbance instability.

(v) *If desired*, use steps *(i)–(iv)* and a search algorithm to establish operational limits based on risk.

A. Uncertainty Modeling

The power system can be considered to consist of a set Γ of uncertain system parameters. Within this paper, this set includes the loading and load power factor at individual buses, power flows through VSC-HVDC lines, and the power output of intermittent renewable sources. It could also include the type of connected load (considering the dynamic response of the load) amongst other uncertainties. Where possible, historical data for the power system being studied can be analyzed to accurately reproduce the stochastic variation of each uncertain parameter $\gamma \in \Gamma$. If required, correlation between different parameters can be accounted for through suitable modelling of the uncertainty distributions (Gaussian or otherwise).

The Monte Carlo process can be used to generate randomly selected operating points. Simulation and linearization of the power system model will provide the critical mode damping values at each of these operating points. From this data, the *pdf* for the critical mode damping can be determined. This *pdf* can subsequently be used in conjunction with measures of severity in order to quantify the risk of small-disturbance stability issues.

B. Quantifying Risk

Risk is related to the probability of an event occurring, and the subsequent severity and consequences of the event [1], [2]. The probability of varying modal locations in the complex plane is determined through the use of the stochastic Monte Carlo sampling. The severity can be defined using a variety of techniques. Perhaps the most valuable approach is the use of economic risk assessment, as it facilitates the comparison of a wide variety of potential system risks on the same (financial) basis. However, there are many complexities surrounding the mitigation of stability issues and it is extremely difficult to apportion the correct economic valuation to the wide variety of control and protection devices which should act to avoid the potentially cataclysmic effects of small-signal rotor angle instability.

Severity is therefore quantified through the use of a technical measure – the settling time for power system oscillations following a disturbance. This measure can be readily tailored by systems operators to suit particularly power systems and the regulations under which they are operated.

1) Oscillation Settling Times

The system dynamic response can be assumed to be of a second-order as described by the critical (the least damped, lowest frequency) electromechanical mode $\lambda = \sigma \pm j\omega$. The oscillations due to higher frequency electromechanical modes, typically with higher damping as well, will quickly attenuate and the overall dynamics will be driven by the least damped mode. For these oscillations the settling time T_S is dependent on the tolerance (*tol.*) and damping (σ) according to (1). Also

provided in (1) is the numerical equation if settling, for example, to within a 5% tolerance of the maximum deviation is required.

$$T_S = \frac{\ln(tol.)}{\sigma} = \frac{\ln(0.05)}{\sigma} = \frac{-3.00}{\sigma} \quad (1)$$

2) Risk Matrix

The use of a risk matrix represents the most easily comprehendible approach to risk assessment – combining discrete probability ranges with discrete severity ranges (oscillation settling times). Such a matrix can be readily designed and adapted for application on any specific practical system. In [17], a five level risk-matrix based on fuzzy logic rules is used to determine a final risk index based on a set of individual indices. The example risk matrix which has been utilized within this study to assess the risk of small-disturbance issues is presented in Fig. 1.

A risk level will be determined for each range of oscillation settling times: *unstable, >60 s, 20–60 s,* and *<20 s*. The system risk level will simply be the highest risk level seen across all groups. The severity and probability ranges presented are only illustrative and should be designed based on permissible oscillation levels for each specific power system.

		Settling Time of Oscillations			
		Unstable	**>60 s**	**20–60 s**	**<20 s**
Probability	**0%**	OK	OK	OK	OK
	0–1%	Moderate	OK	OK	OK
	1–5%	Severe	Moderate	OK	OK
	5–20%	Severe	Moderate	OK	OK
	20–50%	Severe	Severe	Moderate	OK
	50–100%	Severe	Severe	Moderate	OK

Fig. 1. Risk matrix for analysis of probabilistic small-disturbance security assessment results.

3) Continuous Severity Functions

It is also possible to define a continuous severity function $S(\sigma)$, with the risk calculated simply using (2). In (2), $P(\sigma)$ is the probability density function for the mode damping σ. Within this work, the trapezoidal method of numerical integration is used.

$$Risk = \int P(\sigma) S(\sigma)\, d\sigma \quad (2)$$

A number of severity functions have been investigated within this work, depicted in Fig. 2. These functions should be tailored (as a risk matrix would be) to weight specific portions of the modal damping *pdfs* as desired. Simulations are subsequently required in order to define numerical thresholds for acceptable risk levels based on regulatory requirements of system operational performance.

The three functions have been defined and investigated within this study. These are described by (3)–(5) and coefficients have been selected so that all are zero for $\sigma < -0.05$ and have a severity of 1 at the instability boundary. The cutoff at $\sigma < -0.05$ is selected to coincide with the previously define risk matrix (Fig. 1) where *severe* risks are defined only by oscillations lasting longer than 60 s. As with all aspects of the methodology, these coefficients can be customized by the user to represent the desired severity characteristics – with larger values resulting in a greater weighting towards unstable cases.

$$\textit{Stepped:} \quad S(\sigma) = \begin{cases} 0.25 & \text{for } -0.05 \le \sigma < 0, \\ 1 & \sigma \ge 0. \end{cases} \quad (3)$$

$$\textit{Linear:} \quad S(\sigma) = 20(\sigma + 0.05) \text{ for } \sigma \ge -0.05. \quad (4)$$

$$\textit{Quadratic:} \quad S(\sigma) = 400(\sigma + 0.05)^2 \text{ for } \sigma \ge -0.05. \quad (5)$$

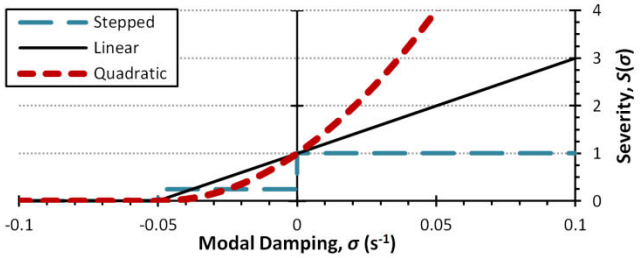

Fig. 2. Continuous severity functions for use with risk-based PSSA.

C. Risk-based Stability Limits

There are many limits and restrictions on the operation of power systems which are typically established using deterministic *worst-case* scenarios. The use of probabilistic approaches to offline system operational studies allows risk-based stability limits to be defined. This will ensure that system assets are not constantly curtailed or underused to mitigate for extremely rare system contingencies.

Once an acceptable risk level is defined (using either a matrix or numerical thresholds based on continuous severity functions), any optimization technique can be used to establish system limits. Within this work, a simple bisecting iterative process is used to set limits on inter-area power transfer based on acceptable exposure to small-disturbance stability risks. Initial operating points are selected and evaluated in order to classify them based on the resulting system risk level, either *acceptable* or *unacceptable*. Once *acceptable* and *unacceptable* limits are established, the space is searched again at the midpoint between these limits. This new operating point is tested and classified as *acceptable* or *unacceptable* and the appropriate limit is redefined. This process of bisecting the search space is repeated until the limit is determined to an appropriate resolution.

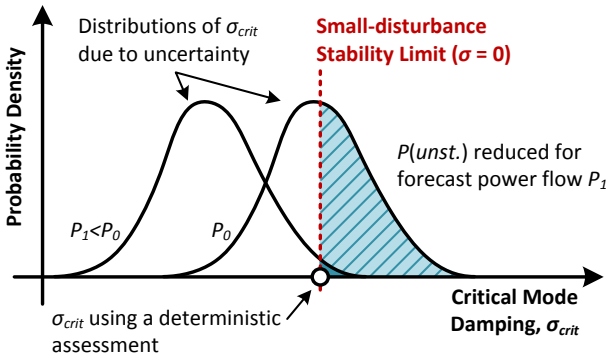

Fig. 3. Illustration of reduction in probability of unstable oscillations when considering a forecast power flow P_1<P_0.

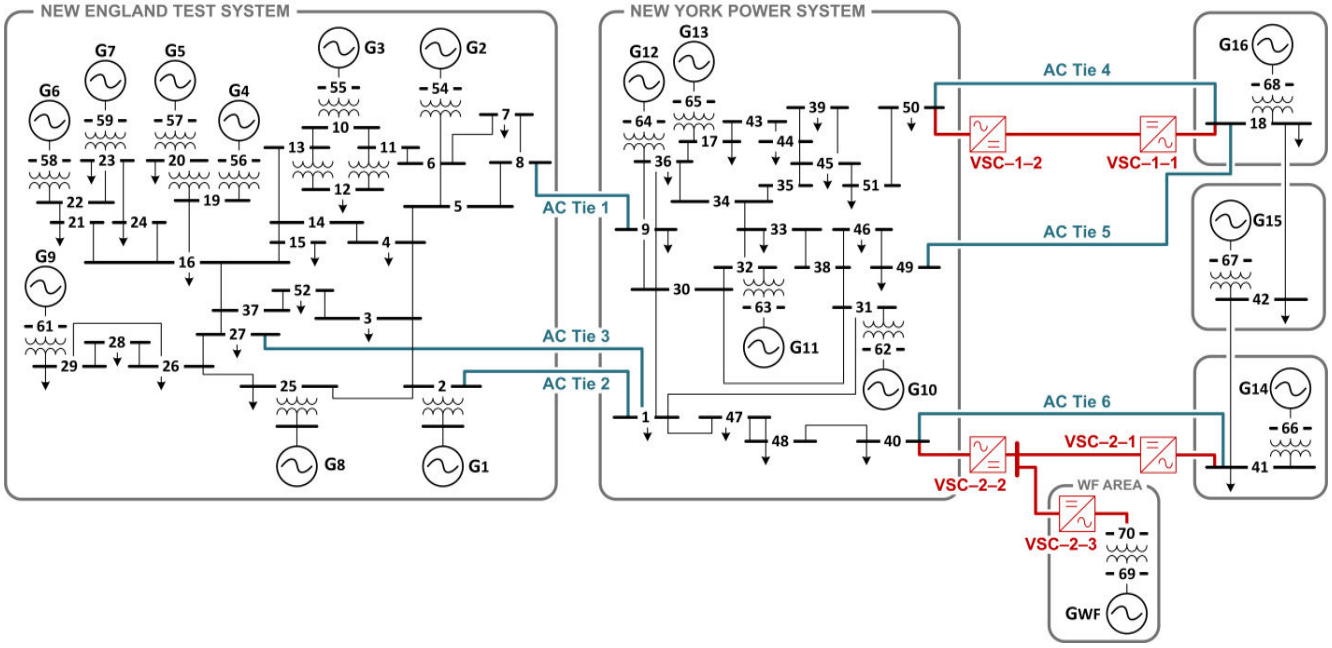

Fig. 4. Modified NETS NYPS test network, including one point-to-point VSC-HVDC line and a three-terminal VSC-MTDC grid incorporating a 500 MW wind farm.

D. Probabilistic Security Margin

The concept of *probabilistic security margins* expands on the use of risk-based limits to more accurately represent the effects of uncertainty on system operation. Security margins (SMs) are deterministic measures of a margin (usually additional loading or line power flow) that can be allowed before reaching an operational limit [18]. As these deterministic measures do not account for the true variability inherent in power system operation, they may result in operating scenarios within the forecast SM that exhibit a high probability of instability. By incorporating uncertainties into the system simulation it is possible to define the probability of small-disturbance system stability associated with various margins. By way of an example, the *99% Probabilistic SM* is defined as the allowable forecast margin within which 99% of operating points will be stable to small disturbances, given the modeled stochastic system variability. An illustration is presented in

Fig. 3 and the concept is demonstrated in the sequel on a test system (both under normal operation and with a line outage contingency).

III. Test System

The methods described within this paper are illustrated using a modified version of the 16 machine, 68 bus reduced order representation of the New England Test System and the New York Power System (NETS & NYPS). The network (including modifications) is shown in Fig. 4. System analysis and simulations are all performed within the MATLAB/Simulink environment making use of modified MATPOWER [19] functions to perform optimal power flows.

A. AC System Details

The generators are controlled as described in [20] with G1–8 under slow DC excitation (IEEE-DC1A), and G9 equipped with a fast acting static exciter (IEEE-ST1A) and a Power System Stabilizer (PSS). The remaining generators (G10–16) are under constant manual excitation. All generators are represented by full sixth order models. System loads are modeled as constant impedance. Other load models can be used without any loss of generality of the proposed methodology. Full system details, generator and exciter parameters are given in [20] with PSS settings for G9 taken from [9]. Additionally, generator G10 (with the NYPS area) has been de-rated from its standard nominal output of 500 MW to 250 MW. Dynamic parameter values have been adjusted to reflect this.

B. VSC-HVDC System Details

Two VSC-HVDC systems have been added to the network to support the most heavily loaded inter-area ties: AC Tie 4 (*line 18–50*) and AC Tie 6 (*line 40–41*). Each converter station is modeled as an injection of active and reactive power [21]. As these studies are concerned with electromechanical oscillations with typical frequencies of 0.2–2.5 Hz, the fast dynamics associated with semiconductor device switching operations are neglected [21]. Converter station controllers are included as described in [22] and DC lines are modeled as presented in [23].

The first system (*VSC–1*) is a point-to-point VSC-HVDC line connected in parallel with AC Tie 4. The converter connected to bus 18 (*VSC–1–1*) regulates the DC voltage. The converter connected at bus 50 (*VSC–1–2*) controls active power injected into the AC systems from the VSC-HVDC line. At both converters, reactive power injection is regulated at zero. This VSC-HVDC system is rated at 800 MW.

The second system (*VSC–2*) is a multi-terminal HVDC (MTDC) system consisting of three converter stations. *VSC–2–1*, connected to bus 41, controls the active power flow from the G14 area into the VSC-MTDC system and is rated at 400 MW. *VSC–2–2* is connected to bus 40 and acts as a slack con-

verter, regulating the DC voltage. This converter is rated sufficiently high to deliver all power to the AC system from the VSC-MTDC grid. The third converter (*VSC–2–3*) is connected to a large wind farm. Active power injected into the MTDC system is determined by the output of this wind farm, and reactive power is supplied as required to support the renewable generation. *VSC–2–3* is rated in order to support maximum active power transfer from the wind farm.

C. Wind Farm System Details

A large 500 MW wind farm (GWF) in connected to the test network through the *VSC–2* MTDC system. For the PSSA studies performed it has been assumed that the power output from the wind farm will be constant during each individual investigated operating point (at which the system is linearized and small-disturbance analysis is completed).

The converter to which the wind farm is connected (*VSC–2–3*) operates using *frequency–AC voltage* control. It has been assumed that the converter is able to maintain a constant AC voltage such that all power produced by the wind farm is transferred to the VSC-MTDC system. This assumption is valid as long as the DC voltage does not deviate considerably. This simplification is acceptable as the work presented is focused on the small-disturbance rotor angle stability of the mixed AC/DC system, and not on the fast transient performance of the VSC-HVDC systems.

D. Operational Constraints

An optimal power flow solution is used within this work to more accurately generate representative system operating points. All voltages are constrained within the range 0.9–1.1 pu, with the exception of G14–16 which are set to 1.0 pu to represent the stiffness of these single machine equivalents of larger networks. Additionally, line constraints are placed on the AC tie-line infeeds from areas G14 and G16 to represent thermal line limits. These are equal to 800, 400, and 600 MVA for AC Ties 4–6 respectively.

IV. PSSA Application

The probabilistic small-disturbance security assessment methods previously outlined have been performed on the test system in order to demonstrate the relevance and applicability of the proposed techniques.

A. Stochastic Variation of System Operating Conditions

The PSSA is completed by considering the stochastic variation of system conditions around their predicted values. For the investigated test system, there are a number of sources of uncertainty. For practical studies, historical data could be used in order to assess the level of uncertainty surrounding forecasted operating scenarios.

1) Loading Uncertainty

A small variation in system loading is considered to represent the possible forecast inaccuracy. Additionally, the probable correlation between the loading levels of various system buses is also modeled. The network loads are categorized as *industrial* or *residential* based on their nominal power factors – all loads with a power factor lower than 0.9 are labeled *industrial*. The correlation coefficients ρ between different loads are as in [24] with $\rho = 0.8$ between *residential* loads, $\rho = 0.4$ between *industrial* loads, and $\rho = 0.2$ between *residential and industrial* loads.

Loads are modeled as being normally distributed with active power mean nominal values, and small standard deviation *(s.d.)* equal to 5% at $3\sigma_\gamma$. The correlation is modeled by sampling from a multivariate normal distribution where the covariance between two loads x and y $\left(\text{cov}(x,y)\right)$ is determined from the desired correlation coefficient $\left(\rho(x,y)\right)$ and the *s.d.* of each load $\left(\sigma_\gamma\right)$ as in (6). Load power factors are non-correlated with *s.d.* of 5% at $3\sigma_\gamma$.

$$\text{cov}(x,y) = \rho(x,y)\left[\sigma_\gamma^2(x)\cdot\sigma_\gamma^2(y)\right]^{1/2} \tag{6}$$

2) VSC-HVDC System Operation Uncertainty

VSC-HVDC system power injection values are modeled based on a probability distribution obtained from the Murraylink 220 MW VSC-HVDC line embedded within the National Electricity Market (NEM) of Australia. This interconnector is utilized as a regulated asset and is operated in parallel with the AC Heywood Interconnector. The data used to build the *pdf* for the VSC-HVDC power flow is sourced from [25] and represents a two month period from January to February 2012 when there were no HVDC outages. Only periods where net flow (in both the Heywood and Murraylink interconnectors) is in the direction of South Australia to Victoria is considered.

This data source has been selected as it is representative of the configuration within the test system – where the VSC-HVDC lines operate in parallel with existing AC ties. The *pdf* for the VSC-HVDC power flow is presented in Fig. 5 where it can be seen that the link is rarely operated at near-rated power and median HVDC power flow through the line is just 0.25 pu. Operational power reference set-points for *VSC–1–2* and *VSC–2–1* are sampled from this distribution. (*Note:* For many power systems though, bidirectional power flow through HVDC line will need to be modelled. In this test system however, the NYPS region is always a net importer of power and so VSC-HVDC export from NYPS would simply result in undesirable loop flows.)

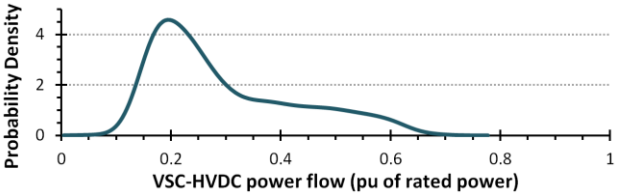

Fig. 5. *Pdf* of VSC-HVDC power flow based on usage data from the Murraylink 220 MW line in the NEM.

3) Wind Farm Generation Uncertainty

Electrical power output from the wind farm (GWF) is determined by the wind speed v. Within this work, v is a random variable sampled from a Weibull probability distribution, as described by (7).

$$f(v)=\begin{cases}\frac{k}{\varphi}\left(\frac{v}{\varphi}\right)^{k-1}e^{-(v/\varphi)^k} & \text{for } v\geq 0,\\ 0 & v<0.\end{cases} \quad (7)$$

In (7), k is the *shape parameter* and φ is the *scale parameter* (commonly signified by λ but called φ here to avoid confusion). In this study, values for these parameters were sourced from [26] with $k=2.2$ and $\varphi=11.1$. The wind farm consists of 100 Areva M5000 5 MW turbines [27]. The total power produced is calculated by selecting a wind speed from the given distribution, determining a single turbine's output according to its power curve, and then scaling the individual turbine output to the capacity of the whole wind farm. More accurate calculation of wind farm output is possible though this would not affect the methodology presented, only the final numerical results.

B. Risk for a Forecasted Operating Scenario

The proposed probabilistic security analysis is completed for two forecasted loading scenarios. 5000 Monte Carlo (MC) simulations are used in each case to evaluate the system risk based on the stochastic variation around the given operating point. If desired, MC variance reduction techniques can be exploited to attempt to reduce the number of simulations required, and stopping rules such as those presented in [11] can be used. The variance reduction techniques however, were not used in this case as the number of simulations was not considered to be excessive for this type of off-line analysis. The scenarios considered represent *(i)* a 2% increase, and *(ii)* a 5% increase in NYPS area loading. Due to the generation and line constraints, almost the entirety of this power is delivered from the NETS area – resulting in increased NETS→NYPS power flow. .

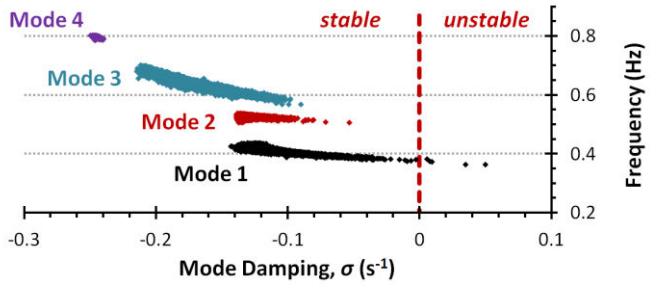

Fig. 6. Distribution of low frequency modes due to stochastic variations for the *2% NYPS increase* forecasted loading scenario.

The system displays four low frequency (<1 Hz) oscillatory electromechanical modes with damping factors below 5%. All other electromechanical modes are adequately damped. The distribution of the low frequency modes for the *2% NYPS increase* case is presented in Fig. 6. It is clearly evident from this plot that Mode 1 (the lowest frequency mode) is the critical mode with respect to system small-disturbance stability and therefore this mode will form the focus of the remainder of the analysis presented.

The *pdf* for the *damping* (real part σ) of Mode 1 for the forecasted NYPS loading increases can be produced from modal distributions using a kernel density estimate [28]. In order to determine the risk surrounding this forecasted scenario, the severity must be also defined. As previously outlined, a technical measure of severity relating unstable or persistent poorly damped power oscillations is used within this work. This can be assessed using a discrete risk matrix such as Fig. 1, or using continuous severity functions $\left(S(\sigma)\right)$, Fig. 2.

1) Risk Matrix

The matrix developed previously has been used to assess the risk of small-disturbance stability issues for the two forecasted scenarios. The resulting *pdfs* of Mode 1 damping shown in Fig. 7 have been colored to represent the risk matrix levels of *OK*, *Moderate*, and *Severe*.

It is clear that the system is exposed to greater risk at the *5% increase* forecast loading scenario, when the system risk level is *Severe*. For the *2% increase* in NYPS loading, the total risk level is *Moderate* with low probabilities of instability or persistent oscillations with settling times greater than 60 s. With NYPS loading increased by 5%, the probability of instability has increased to *severe* levels and the risk matrix provides a quick tool to assess if predefined limits have been exceeded. There may be circumstances where greater distinction is required (between multiple *moderate* scenarios for instance). In these instances, either further information must be provided (such as the calculated probabilities for different severity bands), or more complex severity functions must be used to inform comparative assessments.

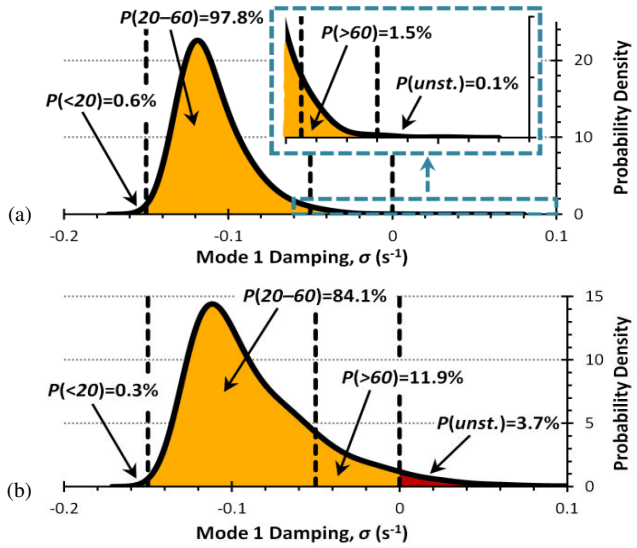

Fig. 7. *Pdf* for critical Mode 1 damping for (a) the *2% NYPS increase*, and (b) the *5% NYPS increase* scenarios (colored to represent risk levels).

2) Severity Functions

The severity functions outlined previously have been used to evaluate the risk measure for the forecasted loading scenario. The risk values produced using these functions should only be compared by considering the values for different scenarios produced by individual severity functions and not *inter-function* comparisons. Plots of $P(\sigma)\times S(\sigma)$ for each severity function are presented in Fig. 8 for the *5% increase* scenario. It is clear that the quadratic function gives far greater weighting to the unstable region of the plot (when $\sigma>0$).

The calculated values of risk according to (2) are given in

Table 1, where it can be seen that all functions result in a clear increase in risk when the NYPS loading level is increased from 2 to 5%. Severity functions can be defined and parameterized to weight different parts of the modal damping *pdfs*. Function selection may influence the perceived level of risk, particularly the change in risk between different scenarios. These functions should therefore be carefully designed according to the specifications of individual operators to provide the desired distinction between different operational scenarios.

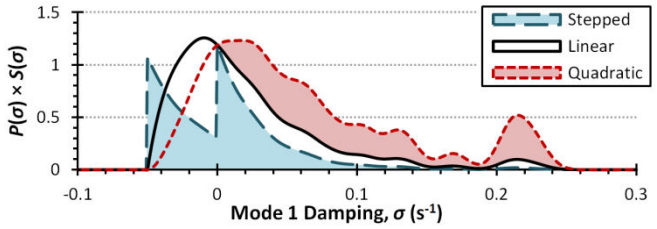

Fig. 8. Evaluation of $P(\sigma)\times S(\sigma)$ for each continuous severity function for the *5% increase* in NYPS loading scenario.

Once numerical limits have been established through system studies, the use of continuous severity functions allows more detailed comparisons of risk levels between varying system contingencies and operating scenarios. This is demonstrated in the following section.

TABLE 1
RISK VALUES FOR LOADING SCENARIOS USING DIFFERENT SEVERITY FUNCTIONS

Scenario	*Risk Values*		
	Stepped	*Linear*	*Quadratic*
2% NYPS increase	0.005	0.005	0.004
5% NYPS increase	0.068	0.110	0.155

C. Risk-based Stability Limit

A risk-based limit on power flow from NETS→NYPS is set using an iterative *divide and conquer* technique and multiple PSSAs. This is initially performed for the system with standard topology, using the matrix from Fig. 1 to define the risk level. The power flow limit is calculated to a precision of 1 MW with a maximum permissible risk level of *moderate*.

The results from the iterative procedure are shown in Fig. 9. It can be seen that the limiting factor is the probability of instability *P*(*unst.*) which is not permitted to exceed 1%. From these results is can be established that a maximum forecast power flow from NETS→NYPS of 1130 MW will ensure that the system risk level does not exceed *moderate*.

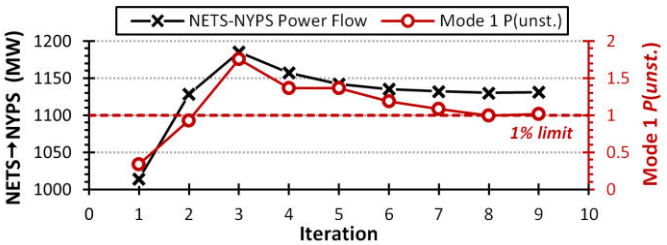

Fig. 9. Iterative process with all lines in service and a maximum allowable risk level of *moderate*.

The risk-based security limit is determined once more, for the contingency when line 1–30 is out of service. It is desired that the system will not be exposed to risks of small-disturbance instability that are greater than when all lines are in service. This procedure is completed by using an alternative, *stepped,* severity function (for illustrative purposes) and the risk measure is evaluated with all lines in service for the maximum flow scenario calculated in the previous example (1130 MW from NETS→NYPS). This provides a limiting system risk value of 0.0249.

The results from this second iterative approach are shown in Fig. 10. The power flow limit for the *line 1–30 out* contingency is 1019 MW. It is clear that with line 1–30 out of service a lower limit on NETS→NYPS power flow is required to maintain the same total system risk level (as measured using the *stepped* severity function).

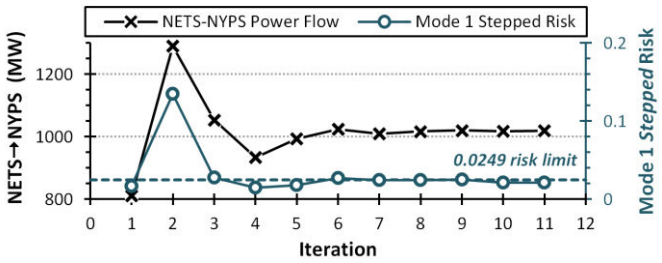

Fig. 10. Iterative process for the *line 1-30 out* contingency with a maximum allowable *stepped* risk value of 0.0249.

D. Probabilistic Security Margin

The determination of risk-based stability limits will ensure that acceptable risk levels are not exceeded during normal system operation. There may be however, instances when it is not possible to avoid exceeding these limits (such as during contingencies or extreme system loading events). In such cases awareness of the extent to which the probabilistic security margin is exceeded would alert system operators to the angular instability that the system may be exposed to. This would therefore guide their actions towards reducing the risk.

The relationship between *P*(*stab.*) and the security margin has been calculated for the system with all lines in service and also for the *line 1–30 out* contingency. These are shown in Fig. 11 where the security margin is calculated relative to the base power flow from NETS→NYPS at the nominal operating point (786 MW).

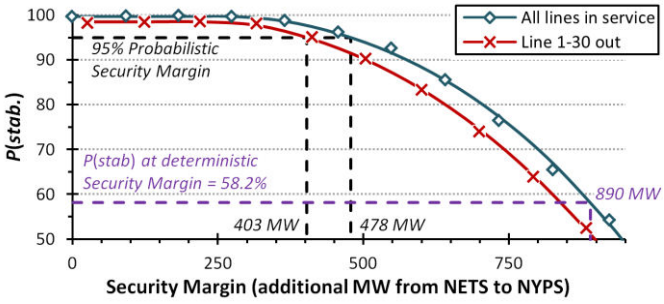

Fig. 11. Relationship between *P*(*stab.*) and security margin.

It can be seen that *P*(*stab.*) is higher for a given NETS→NYPS flow when all lines are in service. By way of illustration, the *95% Probabilistic Security Margin* can be calculated from the plots as 478 MW with all lines in service and 403 MW when line 1-30 is out of service. This margin represents

the allowable increase in NETS→ NYPS flow before $P(stab.)$ decreases below 95%. It should be noted that the deterministic value calculated without considering the system uncertainties suggests a security margin of 890 MW with all lines in service. As shown in Fig. 11, however, at this point $P(stab.)$ is equal to just 58.2% when system variability is considered. This emphasizes importance of probabilistic analysis.

Knowledge of the different probabilistic security margins for various contingencies (or ideally the complete relationship between $P(stab.)$ and security margin as in Fig. 11) would reduce risks when operating under outage contingency conditions. It would enable system control engineers to assess a variety of possible control actions in terms of the risks they introduce and therefore allow more informed decisions.

The probabilistic security margin has been determined and explored in this study in a single dimension (NETS→NYPS power flow) to illustrate the concept. This represents the simplest dimensional projection of otherwise multi-dimensional margin. In practical implementations it may be required to calculate the margin as a function of multiple uncertain parameters using, for example, operational search space characterization such as employed in [29], [30]. This would result in a multi-dimensional hyperplane margin which could be *flattened* (or projected) to any desired parameter for illustration (graphical representation) and further application. Irrespectively of the number of parameters used to define this hyperplane margin, the visualization of the margin would be dimensionally limited due to the restriction of graphical representation.

V. Conclusions

The risk-based probabilistic small-disturbance security assessment methodology proposed within this paper is a novel extension of current dynamic security assessment (DSA) techniques. It has been used successfully with a number of technical severity measures based on oscillation settling time or instability within the work presented. The combination of probabilistic small-disturbance security analysis with risk analysis, particularly with readily understandable risk matrices, can be used to provide guidance to systems operators about potentially problematic scenarios which may emerge.

The PSSA has also been used to determine risk-based inter-area forecast power flow limits for the first time. By combining the PSSA with an iterative process and a risk-based threshold, constraints have been established which ensure acceptable risk levels are not exceeded. The risk threshold can be described using any severity measure and has been demonstrated within this work using both a risk matrix and a continuous function. It has been shown that contingency-specific limits can be determined which maintain the total system risk level for any given operational topology. Furthermore, a new probabilistic security margin has been defined and illustrated within this work to more accurately represent the variable nature of power systems and the uncertainty surrounding forecast operating scenarios.

This work has demonstrated the importance of probabilistic security analysis and risk assessment assessing the small-disturbance stability of power systems. There would be great benefits to be gained by completing such analyses online for projected operating points, guiding systems operation. The techniques proposed however are computationally intensive and, when using a purely numerical (MC) approach, may not be possible for online application. The use of efficient sampling techniques, such as the probabilistic collocation method [31] or the point estimate method [32], or analytical techniques such as [7], may enable sufficient computational savings to allow online application. If such methods are used, the accuracy of the results must be thoroughly verified.

Finally, the presented risk-based analysis could also provide a framework for robust assessment of damping controllers and facilitate risk-based controller design to reduce the *risk* of small-disturbance instability.

References

[1] M. Ni, J. D. McCalley, V. Vittal, and T. Tayyib, "Online risk-based security assessment," *IEEE Trans. Power Syst.*, vol. 18, no. 1, pp. 258–265, Feb. 2003.

[2] H. Wan, J. D. McCalley, and V. Vittal, "Risk based voltage security assessment," *IEEE Trans. Power Syst.*, vol. 15, no. 4, pp. 1247–1254, 2000.

[3] Y. Ou and C. Singh, "Assessment of available transfer capability and margins," *IEEE Trans. Power Syst.*, vol. 17, no. 2, pp. 463–468, May 2002.

[4] M. J. Laufenberg and M. A. Pai, "A new approach to dynamic security assessment using trajectory sensitivities," *IEEE Trans. Power Syst.*, vol. 13, no. 3, pp. 953–958, 1998.

[5] K. Sun, S. Likhate, V. Vittal, V. S. Kolluri, and S. Mandal, "An Online Dynamic Security Assessment Scheme Using Phasor Measurements and Decision Trees," *IEEE Trans. Power Syst.*, vol. 22, no. 4, pp. 1935–1943, Nov. 2007.

[6] D. Ruiz-Vega and M. Pavella, "A comprehensive approach to transient stability control: part II-open loop emergency control," *IEEE Trans. Power Syst.*, vol. 18, no. 4, pp. 1454–1460, Nov. 2003.

[7] A. Dissanayaka, U. D. Annakkage, B. Jayasekara, and B. Bagen, "Risk-Based Dynamic Security Assessment," *IEEE Trans. Power Syst.*, vol. 26, no. 3, pp. 1302–1308, Aug. 2011.

[8] S. M. Ustinov, J. V. Milanović, and V. A. Maslennikov, "Inherent dynamic properties of interconnected power systems," *Int. J. Electr. Power Energy Syst.*, vol. 24, no. 5, pp. 371–378, Jun. 2002.

[9] G. Rogers, *Power System Oscillations*. Norwell: Kluwer Academic Publishers, 2000.

[10] F. Howell, P. Kundur, and C. Y. Chung, "A tool for small-signal security assessment of power systems," in *pica 2001. Innovative Computing for Power - Electric Energy Meets the Market. 22nd IEEE Power Engineering Society. International Conference on Power Industry Computer Applications (Cat. No.01CH37195)*, pp. 246–252.

[11] J. L. Rueda, D. G. Colome, and I. Erlich, "Assessment and Enhancement of Small Signal Stability Considering Uncertainties," *IEEE Trans. Power Syst.*, vol. 24, no. 1, pp. 198–207, 2009.

[12] C. K. Pans, Z. Y. Dong, P. Zhang, and X. Yin, "Probabilistic analysis of power system small signal stability region," in *International Conference on Control and Automation. ICCA '05.*, 2005, vol. 1, pp. 503–509.

[13] R. Arrieta, M. A. Rios, and A. Torres, "Contingency Analysis and Risk Assessment of Small Signal Instability," *Power Tech, 2007 IEEE Lausanne*. pp. 1741–1746, 2007.

[14] M. A. Rios, R. Arrieta, and A. Torres, "Angular Instability 'Day Ahead' Risk Forecasting - Probabilistic Dependency on Load," *IEEE Lat. Am. Trans.*, vol. 5, no. 8, pp. 585–590, 2007.

[15] J. Rueda and I. Erlich, "Probabilistic framework for risk analysis of power system small-signal stability," *Proc. Inst. Mech. Eng. Part O J. Risk Reliab.*, vol. 226, no. 1, pp. 118–133, 2012.

[16] R. Preece and J. V. Milanovic, "Assessing the risk of small disturbance instability in mixed AC/DC networks," in *IREP Symposium Bulk Power System Dynamics and Control IX*, 2013, pp. 1–8.

[17] O. Ruhle and E. Lerch, "Ranking of system contingencies in DSA

systems - first experiences," in *IEEE PES General Meeting*, 2010, pp. 1–6.

[18] Y. V. Makarov, P. Du, S. Lu, T. B. Nguyen, X. Guo, J. W. Burns, J. F. Gronquist, and M. A. Pai, "PMU-Based Wide-Area Security Assessment: Concept, Method, and Implementation," *IEEE Trans. Smart Grid*, vol. 3, no. 3, pp. 1325–1332, Sep. 2012.

[19] R. D. Zimmerman, C. E. Murillo-Sanchez, and R. J. Thomas, "MATPOWER: Steady-State Operations, Planning, and Analysis Tools for Power Systems Research and Education," *IEEE Trans. Power Syst.*, vol. 26, no. 1, pp. 12–19, Feb. 2011.

[20] B. Pal and B. Chaudhuri, *Robust Control in Power Systems*. New York: Springer Inc., 2005.

[21] H. F. Latorre, M. Ghandhari, and L. Söder, "Active and reactive power control of a VSC-HVdc," *Electr. Power Syst. Res.*, vol. 78, no. 10, pp. 1756–1763, Oct. 2008.

[22] R. Preece, J. V. Milanovic, A. M. Almutairi, and O. Marjanovic, "Probabilistic Evaluation of Damping Controller in Networks With Multiple VSC-HVDC Lines," *IEEE Trans. Power Syst.*, vol. 28, no. 1, pp. 367–376, Feb. 2013.

[23] S. Cole, J. Beerten, and R. Belmans, "Generalized Dynamic VSC MTDC Model for Power System Stability Studies," *IEEE Trans. Power Syst.*, vol. 25, no. 3, pp. 1655–1662, Aug. 2010.

[24] W. Li and R. Billinton, "Effect of bus load uncertainty and correlation in composite system adequacy evaluation," *IEEE Trans. Power Syst.*, vol. 6, no. 4, pp. 1522–1529, 1991.

[25] GLOBAL-ROAM, "NEM-Watch." www.NEM-WATCH.info, 2013.

[26] J. P. Coelingh, A. J. M. van Wijk, and A. A. M. Holtslag, "Analysis of wind speed observations over the North Sea," *J. Wind Eng. Ind. Aerodyn.*, vol. 61, no. 1, pp. 51–69, Jun. 1996.

[27] Areva Wind GmbH, "M5000 Technical Data," 2010.

[28] A. W. Bowman and A. Azzalini, *Applied Smoothing Techniques for Data Analysis*. New York: Oxford University Press, 1997.

[29] I. Genc, R. Diao, and V. Vittal, "Decision tree-based preventive and corrective control applications for dynamic security enhancement in power systems," *IEEE Trans. Power Syst.*, vol. 25, no. 3, pp. 1611–1619, 2010.

[30] C. Singh and J. Mitra, "Composite system reliability evaluation using state space pruning," *IEEE Trans. Power Syst.*, vol. 12, no. 1, pp. 471–479, 1997.

[31] R. Preece, N. C. Woolley, and J. V. Milanovic, "The Probabilistic Collocation Method for Power System Damping and Voltage Collapse Studies in the Presence of Uncertainties," *IEEE Trans. Power Syst.*, vol. 28, no. 3, pp. 2253–2262, 2013.

[32] X. Xu, T. Lin, and X. Zha, "Probabilistic analysis of small signal stability of microgrid using point estimate method," in *2009 International Conference on Sustainable Power Generation and Supply*, 2009, pp. 1–6.

Robin Preece (GS'10, M'13) received his BEng degree in Electrical and Electronic Engineering in 2009 and his PhD degree in 2013, both from the University of Manchester, United Kingdom. He is currently working as a Research Associate at the same institution investigating risk and uncertainty with respect to the stability of future power systems.

Jovica V. Milanović (M'95, SM'98, F'10) received his Dipl.Ing and his MSc degrees from the University of Belgrade, Yugoslavia, his PhD degree from the University of Newcastle, Australia, and his Higher Doctorate (DSc degree) from The University of Manchester, UK, all in Electrical Engineering. Currently, he is a Professor of electrical power engineering and Deputy Head of the School of Electrical and Electronic Engineering at The University of Manchester (formerly UMIST), UK, Visiting Professor at the University of Novi Sad, Novi Sad, Serbia and Conjoint Professor at the University of Newcastle, Newcastle, Australia.